Electroluminiscencia y amplificación óptica en nanoestructuras de silicio: hacia la integración de la electrónica y la fotónica

Electroluminiscence and optical amplification in silicon nanostructures: towards the integration of electronics and photonics

Blas Garrido

EME, Departamento de Electrónica, Universidad de Barcelona. Email: blas@el.ub.es

RESUMEN

La línea de investigación de mi equipo pretende establecer una plataforma tecnológica de silicio en el campo de la fotónica, con objeto de desarrollar un amplio conjunto de aplicaciones. En particular, la fotónica de silicio carece todavía de una fuente de luz eficiente e integrable, como por ejemplo un LED o un láser. Recientemente, la utilización de nanocristales en óxidos de silicio o matrices de nitruros se han demostrado como materiales competitivos tanto para componentes activos (emisores de luz controlados electrónicamente y ópticamente), como pasivos (gías de onda y moduladores) El objetivo final es obtener una integración completa de las funciones electrónicas y ópticas en el mismo chip CMOS. La primera parte de este trabajo introducirá las propiedades ópticas y estructurales de LEDs fabricados con nanoestructuras de silicio. La segunda parte tratará la interacción de estos nanocristales con elementos de tierras raras (Er), que permiten un sistema híbrido eficiente de emisión en la tercera ventana de las fibras ópticas. Presentaré la fabricación de amplificadores para guías de onda ópticas en 1,54 µm, para los cuales hemos demostrado recientemente una ganancia óptica en guías ópticas hechas con materiales subóxidos de silicio.

Palabras clave: Electroluminiscencia, Amplificadores Opticos, Nanoestructuras de Silicio.

ABSTRACT

This line of research of my group intends to establish a Silicon technological platform in the field of photonics allowing the development of a wide set of applications. Particularly, what is still lacking in Silicon Photonics is an efficient and integrable light source such an LED or laser. Nanocrystals in silicon oxide or nitride matrices have been recently demonstrated as competitive materials for both active components (electrically and optically driven light emitters and optical amplifiers) and passive ones (waveguides and modulators). The final goal is the achievement of a complete integration of electronic and optical functions in the same CMOS chip. The first part of this paper will introduce the structural and optical properties of LEDs fabricated from silicon nanostructures. The second will treat the interaction of such nanocrystals with rare-earth elements (Er), which lead to an efficient hybrid system emitting in the third window of optical fibers. I will present the fabrication and assessment of optical waveguide amplifiers at 1.54 µm for which we have been able to demonstrate recently optical gain in waveguides made from sputtered silicon suboxide materials.

Key words: Electroluminescence, Optical Amplifiers, Silicon Nanoestructures.

REFERENCIAS Y ENLACES

[1] T. S. Iwayama, N. Kurumado, D. E. Hole, P. D. Townsend, "Optical properties of silicon nanoclusters fabricated by ion implantation", *J. Appl. Phys*. **83**, 6018-6022 (1998).

[2] B. Garrido, M. López, O. González, A. Pérez-Rodríguez, J. R. Morante, **“**Correlation between structural and optical properties of Si nanocrystals embedded in SiO_2: The mechanism of visible light emission”, *Appl. Phys. Lett*. **77**, 3143-3145 (2000).

[3] F. Iacona, C. Bongiorno, C. Spinella, S. Boninelli, F. Priolo, **“**Formation and evolution of luminescent Si nanoclusters produced by thermal annealing of SiO_x films”, *J. Appl. Phys*. **95**, 3723-3732 (2004).

[4] K. S. Cho, N.-M. Park, T.-Y. Kim, K.-H. Kim, G. Y. Sun**g,** J. H. Shin, **“**High efficiency visible electroluminescence from silicon nanocrystals embedded in silicon nitride using a transparent doping layer”, *Appl. Phys. Lett.* **86**, 071909 (2005).

[5] B.-H. Kim, C.-H. Cho, T.-W. Kim, N.-M. Park, G. Y. Sung, S.-J. Park, “Photoluminescence of silicon quantum dots in silicon nitride grown by NH_3 and SiH_4**”**, *Appl. Phys. Lett.* **86**, 091908 (2005).

[6] L. N. Dinh, L. L. Chase, M. Balooch, W. J. Siekhaus, F. Wooten, **“**Optical properties of passivated Si nanocrystals and SiO_x nanostructures”, *Phys. Rev. B* **54**, 5029-5037 (1996).

[7] K. Luterová, I. Pelant, J. Valenta, J. L. Rehspringer, D. Muller, J. J. Grob, J. Dian, B. Hönerlange**, “**Red electroluminescence in Si^+-implanted sol–gel-derived SiO_2 films”, *Appl. Phys. Lett.* **77**, 2952-2954 (2000).

[8] J. De La Torre, A. Souifi, A. Poncet, C. Busseret, M. Lemiti, G. Bremond, G. Guillot, O. González, B. Garrido, J. R. Morante, C. Bonazos, “Optical properties of silicon nanocrystal LEDs“, *Physica E* **16**, 326-330 (2003).

[9] A. Irrera, F. Iacona, G. Franzo, S. Boninelli, D. Pacifici, M. Miritello, C. Spinella, D. Sanfilippo, G. Di Stefano, P. G. Fallica, F. Priolo, “Correlation between electroluminescence and structural properties of Si nanoclusters”, *Opt. Mater*. **27**, 1031-1040 (2005).

[10] D. J. Di Maria, J. R. Kirtley, E. J. Pakulis, D. W. Dong, T. S. Kuan, F. L. Pesavento, T. N. Theis, J. A. Cutro, S. D. Brorson, “Electroluminescence studies in silicon dioxide films containing tiny silicon islands”, *J. Appl. Phys.* **56**, 401 (1984).

[11] R. J. Walters, H. Atwater, G. Bourianoff, “Field-effect electroluminescence in silicon nanocrystals”, *Nat. Mater.* **4**, 143-146 (2005).

[12] B. Garrido, J. Samitier, J.R. Morante, J. Monserrat, C. Domínguez, “Configurational statistical model for the damaged structure of silicon oxide after ion implantation”, *Phys. Rev. B* **49**, 14845-14849 (1994).

[13] M. Perálvarez, M. López, B. Garrido, J. R. Morante, J. Barreto, V. J. Cadarso, M. Riera, K. Zinoviev, C. Domínguez, “Precipitation of highly luminescent phases from PECVD Si suboxides”, *Mat. Res. Soc. Symp. Proc.* **832**, F.27 (2005).

[14] O. González-Varona, B. Garrido, S. Cheylan, A. Pérez-Rodríguez, A. Cuadras, J. R. Morante, “Control of tunnel oxide thickness in Si-nanocrystal array memories obtained by ion implantation and its impact in writing speed and volatility”, *Appl. Phys. Lett*. **82**, 2151-2153 (2003).

[15] J. Linnros, N. Lalic, A. Galeckas, V. Grivickas, “Analysis of the stretched exponential photoluminescence decay from nanometer-sized silicon crystals in SiO_2”, *J. Appl. Phys*. **86**, 6128-6134 (1999).

[16] E. Kameda, T. Matsuda, Y. Emura, T. Ohzone, “Fowler–Nordheim tunneling in MOS capacitors with Si-implanted SiO_2”, *Solid State Electron.* **42**, 2105-2111 (1998),

[17] H. S. Han, S. Y. Seo, J. H. Shin, “Optical gain at 1.54 µm in erbium-doped silicon nanocluster sensitized waveguide”, *Appl. Phys. Lett*. **79**, 4568-4570 (2001).

[18] H. S. Han, S.Y. Seo, J. H. Shin, N. Park, “Coefficient determination related to optical gain in erbium-doped silicon-rich silicon oxide waveguide amplifier”, *Appl. Phys. Lett.* **81**, 3720-3722 (2002).

[19] J. Lee and J. H. Shin, N. Park, “Optical Gain at 1.5 µm in Nanocrystal Si-Sensitized Er-Doped Silica Waveguide Using Top-Pumping 470 nm LEDs”, *J. Lightwave Technol.* **23**, 19-24 (2005).

[20] N. Daldosso, D. Navarro-Urrios, M. Melchiorri, L. Pavesi, F. Gourbilleau, M. Carrada, R. Rizk, C. Garcia, P. Pellegrino, B. Garrido, L. Gognolato, “Absorption cross section and signal enhancement in Er-doped Si nanocluster rib-loaded waveguides”, *Appl.Phys.Lett*. **86**, 261103 (2005).

[21] H. Mertens, A. Polman, I. M. P. Aarts, W. M. M. Kessels, M. C. M. Van de Sanden, “Absence of the enhanced intra-4*f* transition cross section at 1.5 μm of Er^{3+} in Si-rich SiO_2”, *Appl.Phys.Lett*. **86**, 241109 (2005).

1. Electroluminescence from Si-based LEDs

Si nanocrystals (Si-nc) in transparent dielectric matrices, such as SiO2 and SiNx, have been revealed as efficient and robust light emitters and represent the most promising active materials for optoelectronic devices in Si technology [1-5]. Among the different approaches to synthesize the Si-nc [1-7], ion implantation is the most widely used but PECVD has been demonstrated as an interesting alternative as thick layers of silicon rich silicon oxide (SRSO) with uniform Si-excess can be grown routinely [3]. Figure 1 shows TEM micrographs of Si-nc obtained by us by using ion implantation of Si in SiO_2.

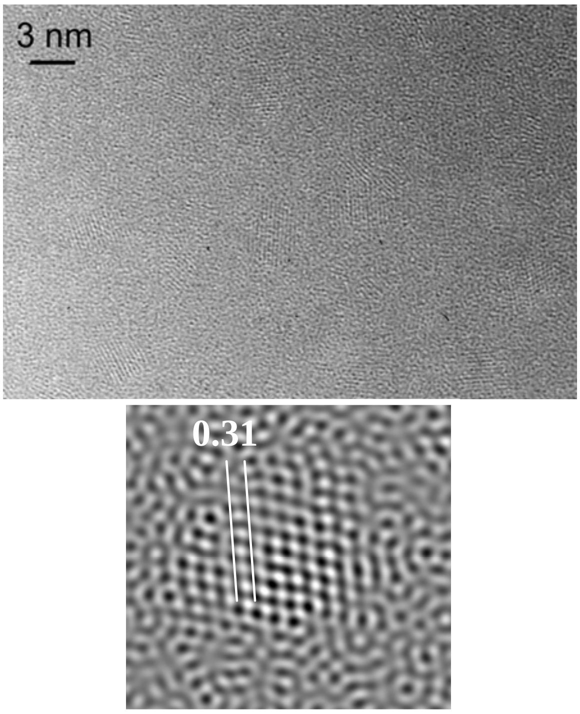

Fig. 1. Si nanocrystals formed by ion implantation

Several authors have reported electro-luminescence (EL) from MOS light emitting diodes (LEDs) based on Si-nc/SiO2 materials [7-10], most of them working under direct current (DC) polarization. The carrier injection in devices with thick SRSO layers proceeds through Fowler-Nordheim (F-N) tunneling and requires the application of high voltages. Under this regime, the charge transport in the oxide takes place via hot-electrons and the electron-hole pairs are generated by impact ionization of the Si-nc [9]. Hot electron transport leads to a fast degradation of the oxide matrix and a low device endurance. In our previous studies [8], we observed that a reduction of the oxide thickness avoids the impact ionization and favours the creation of excitons by simultaneous injection of electrons and holes from opposite contacts. Nevertheless those devices (with SRSO of ~12 nm) showed very low external quantum efficiencies as most of the current was tunnelling assisted by the Si-nc and failed to create excitons. Figure 2 shows some facts of these first devices.

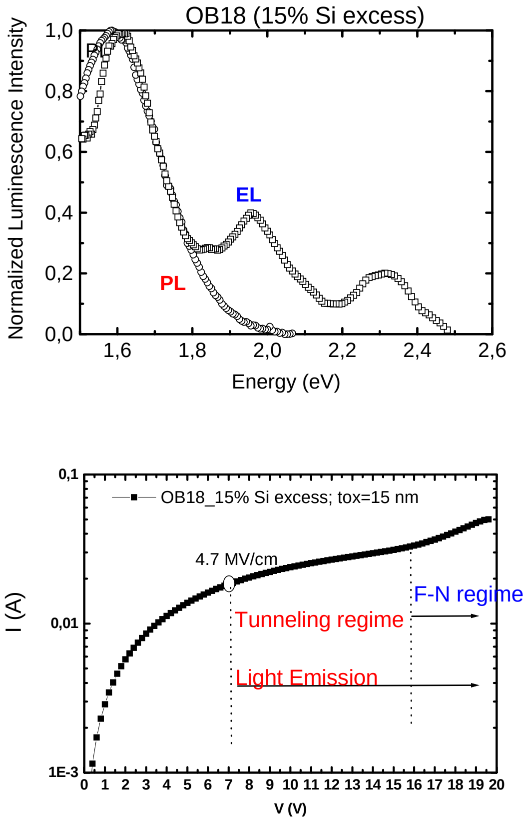

Fig. 2. Spectral emission and I-V of the first continuous LEDs

R. J. Walters *et al.* [11] reported a very promising innovation introducing the concept of alternate injection in which electron and holes were sequentially injected into the Si-nc from the substrate by alternate polarization. Those field emission (FE-LED) devices were obtained by implantation of Si ions into thermally grown SiO_2. However, it is desirable to move to continuous layers, such as PECVD ones, which provide a flat profile of Si excess and a lower amount of defects specially at the interface (tails of the implantation profile).

We have recently obtained FLEDs with high emission efficiency. The device structure is a MOS capacitor with Si-nc embedded in the SiO_2. The SRSO layers were deposited on a p-type Si-substrate by a PECVD reactor using pure silane and nitrous oxide as reaction precursors. The phase separation was achieved by submitting the SRSO layers to high temperature (1250 ºC) annealing in N2 atmosphere during 1 h. Detailed studies showed that photoluminescence (PL) was maximized for a 17% Si atomic excess. We found that this gives rise to very uniform Si-nc distribution with a mean nc-size of about 3.6 nm and an estimated density of ~5·10^17 Si-nc/cm3. N-doped semitransparent polycrystalline silicon (poly-Si) 250 nm thick was deposited as a contact layer. Transmittance spectra show that the poly-Si contacts have a transmission of ~48% in the region of interest (1.4 eV – 1.8 eV). At the onset of the negative voltage pulse (figure 3) an accumulation layer of holes is created at the interface between the SRSO and the substrate. If the driving voltage is large enough, then part of these holes are injected into the Si-nc. At the fall edge of the polarisation pulse (voltage drops back to zero, figure 3), two contributions to the current transient are observed with different fall-times. The faster one can be assigned to the depletion of holes from the accumulation layer (discharge of the capacitor). The slow contribution has a characteristic time of several µs (figure 3b) and is the one correlated with the EL emission; so, we assign this current to the creation of an inversion layer of electrons at the interface between the SRSO and the substrate. Consequently, the Coulomb field created by the positively-charged Si-nc stimulates the injection of electrons from the substrate to the Si-nc, creating excitons inside. It is worth noting that the alternate injection mechanism only involves the Si-nc located relatively close to substrate so hot electron transport and impact ionization are avoided. Therefore, under these operation conditions the reliability of the device is considerably improved. Figure 3 shows the time-resolved measurements of the excitation pulse (a), the current transient at the load resistor (b) and, finally, the EL (c). The curves are represented at the excitation pulse fall-edge, i.e. when the second carrier injection takes place. Comparing the EL emission and the current transient it becomes clear that the EL emission starts once the depletion of holes has been produced (after the fast current component, ~80 ns) and is triggered by the formation of the electron inversion layer caused by the slow component of the current. The calculated fall-time is ~5µs, with a dispersion parameter β of about ~0.6. We have also estimated the external (plug-in) efficiency of our LEDs by carefully calibrating our set-up and the photomultiplier with a commercial LED. We obtain typical values of 0.03 %. Measurements in reference capacitors of the same batch without Si-nc show that using a suitable control oxide the leakage current can be reduced in such a way that the external efficiency would increase by a factor of more than 300, i.e., up to 9%. Furthermore, this is not an intrinsic limitation, as reducing the series resistance (geometrical plus contact) which is of about 80 Ω, will reduce power losses and further increase emission efficiency.

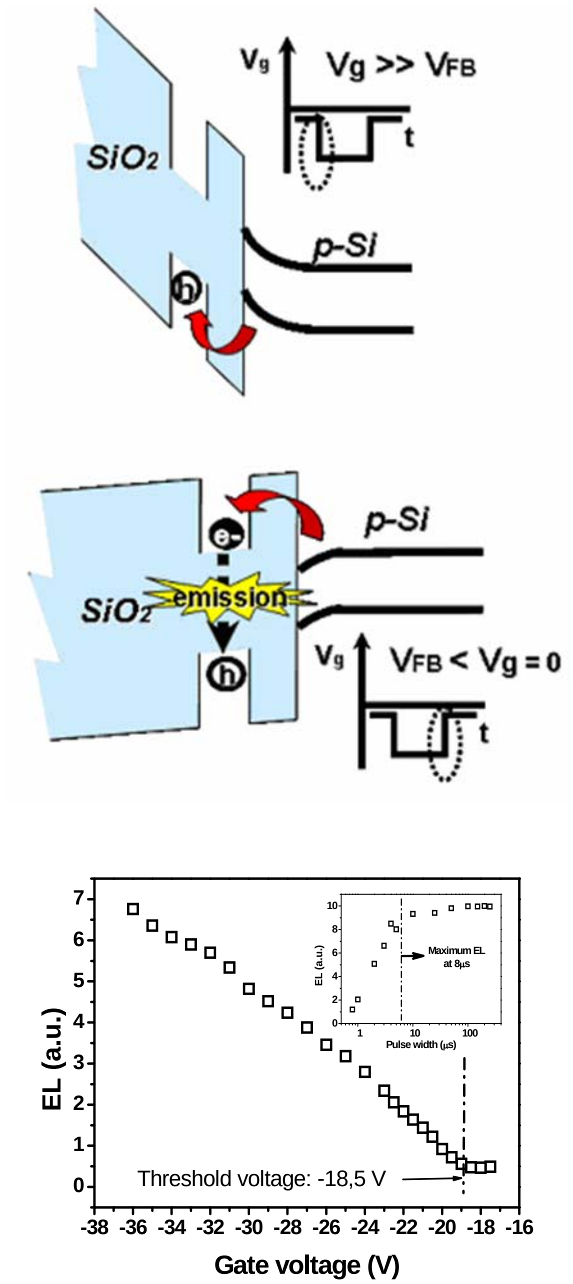

Fig. 3. Schematic representation of injection and EL intensity versus voltage of the FLEDs.

2. Optical amplification in waveguides with Si-nc plus Er

There is a great potential of the material Er-doped SiO_x as a material well adapted for optical amplification, due to the fact that the effective cross-section for absorption increases more than 3 orders of magnitude and the spectra is broad so that cheap LEDs can be used to pump the waveguides instead of expensive lasers as is done in the EDFAs. The material in itself has been the subject of many studies, so far only a few groups have actually fabricated optical waveguides with Er-doped SiO_x as the active layer and studied its amplification properties, in fact Shin and co-workers and us. Shin and co-workers claimed to have observed high optical gain in several SiO_x:Er waveguides [17-19] even, in one case, while optically pumping with a LED. They reported a Signal Enhancement ($I_{pumpON}/I_{pumpOFF}$) between 1.9 dB/cm and 3.5 dB/cm was reported in the range comprised between 1.51 and 1.56 microns, for a pump flux of 1.5 W/cm^2, when pumping from the top with the 477 nm line of an Argon laser.

Regarding our own investigations, in the framework of the European Project Sinergia different waveguides containing Er-doped SiO_x were fabricated and characterized, both by PECVD and Sputtering, with different Si excess and Er content. All samples were studied for optical losses, and it was found that the losses increased with the refractive index, due to the stronger scattering effects induced by a greater index contrast with the SiO_2. The Si content was thus reduced and the deposition parameters and annealing processes were finely tuned in order to improve the waveguide losses, which in the end attained values as low as 0.7 dB/cm. Only the samples showing relatively low losses were finally subjected to pump & probe experiments to determine their potential as optical amplifiers. This section reports some of the most interesting results obtained in these studies. The samples from which we have waveguides are:

Sample label	**Annealing time**	**Thickness**	**Refractive index**
A109	60’	750 nm	1.531
A127	30’	840 nm	1.501
A165	10’	855 nm	1.482
A166	5’	890 nm	1.468
A167	1’	880 nm	1.463

Table I. Thickness and refractive index of the samples studied .

A series of strip-loaded waveguides were fabricated with those materials. Optical lithography and reactive ion etching were used to define the ribs on a SiO_2 cladding deposited on top of the active layers. Two photolithography masks were used for waveguide definition. Next table with the data for the best waveguides. Figure 4 shows some micrographs and 5 the guided modes.

Sample	A108 (A109)	A127	A129 (A165)
Core layer (nm)	750	840	855
SiO_2 top cladding (nm)	1800	1000	1000
Etching depth (nm)	1600	340	310
Refractive index	1.531	1.501	1.482
G	0.55	0.48	0.30
Length (cm)	3	2	1.8

Table II. Physical parameters of the waveguides grown on the different samples.

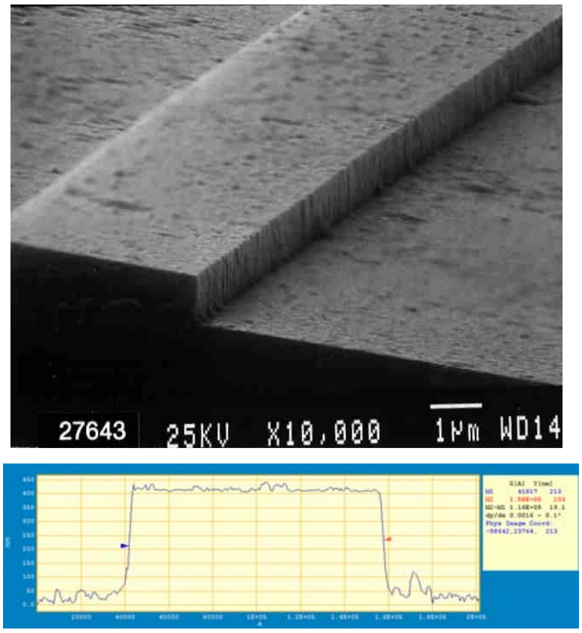

Fig.4. SEM and AFM profile of a rib-loaded waveguide

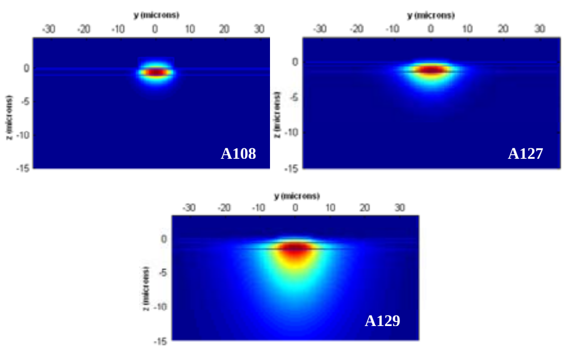

Fig. 5. Simulated fundamental modes in the fabricated 6 m-wide waveguides in sample A108 and 10 m-wide waveguides in samples A127 and A129.

For measuring losses we used as signal source the telecomm laser, which emitted up to 6 mW in the range 1500 nm-1600 nm. Light was coupled into the waveguides through a tapered fibre. We could apply the cut back method as we lack of samples for them. We therefore resorted to measuring total losses. The result of the measurement at different wavelengths in a typical 6 μm wide waveguide is reported in Fig. 6. By subtracting the baseline to the data, a maximum Er-related absorption of 15 dB can be determined, at a wavelength of 1.533 μm. Dividing by the length of the waveguide (3 cm), the Er-related absorption coefficient can be estimated for all wavelengths.

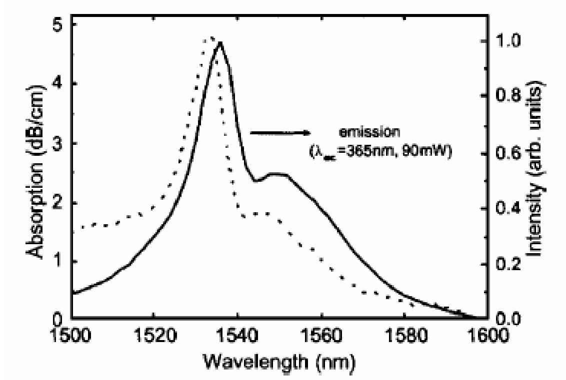

Fig. 6. Losses related to Erbium absorption (dotted line), plotted alongside the PL emission of the sample (continuous line).

$$\alpha(dB) = 4.34 \times N_{Er} \times \Gamma \times \sigma \times L \rightarrow$$
$$\sigma = \frac{\alpha}{4.34 \times N_{Er} \times \Gamma \times L} = 5 \times 10^{-21}\, cm^2$$

This value, which is also that of the stimulated emission cross-section, corresponds to that of Er in SiO_2, and contradicts previous reports by Polman *et al.* and Shin *et al.*, which stated that these cross-sections in SiO_x were increased by one order of magnitude with respect to their value in SiO_2. The maximum gain, being equal to the Er-related absorption, is of 5 dB/cm. The fact that losses of only 2 dB/cm must be overcome means that, in the event that total inversion could be attained, these waveguides could still supply a net optical gain of 3 dB/cm, a higher value than in most available EDWAs [17-21].

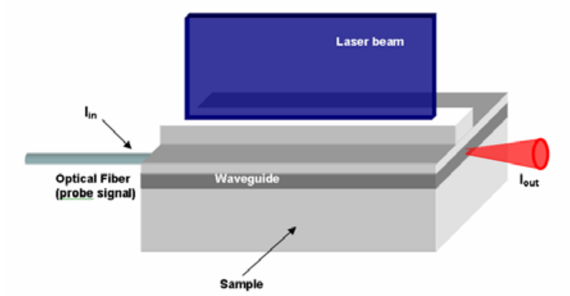

Fig. 7.. Schematic representation of a pump & probe experiment with pumping from the top.

So, we determined the dependence of optical amplification with the signal wavelength. The pump was set at high power (8×10^{21} phot/cm^2·s), while the probe wavelength was varied between 1.525 μm and 1.550 μm, at a fixed pump power of 0.2 mW at laser exit. The corresponding SE values are plotted in Fig. 8, together with the normalized emission spectrum for the Erbium. Amplification takes place exclusively for wavelengths that fall within the peak of emission of the Erbium, between 1.53 μm and 1.54 μm, where the stimulated emission is strong enough to overcome the carrier absorption. The fact that no signal enhancement is observed outside this range confirms the validity of our results, completely excluding the possibility that the increase in signal could be due to anything other than stimulated emission by Erbium ions.

Recently, improved values of signal enhancement and gain have obtained in new sets of samples

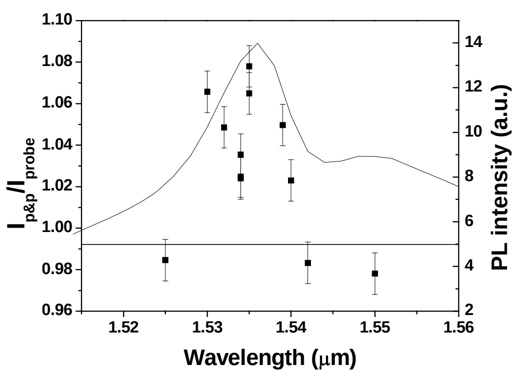

Fig.8. Dependence of the Signal Enhancement with the wavelength of the probe signal, superimposed to a photo-luminescence spectra of the sample. Clearly, the signal is enhanced exclusively for wavelengths that lay within the peak of emission.